Effects of Pulsed Laser Micro Polishing on Microstructure and Mechanical Properties of S7 Tool Steel

ICOMM 2014 No. 103

Justin D. Morrow[1], Qinghua Wang[2], Neil A. Duffie[3], Frank E. Pfefferkorn[4]

[1]Justin D. Morrow; Mechanical Engr., University of Wisconsin – Madison; email: jdmorrow@wisc.edu
[2] Qinghua Wang; Mechanical Engr., University of Wisconsin – Madison; email: qwang232@wisc.edu
[3] Neil A. Duffie; Mechanical Engr., University of Wisconsin – Madison; email: duffie@engr.wisc.edu
[5]Frank E. Pfefferkorn; Mechanical Engr., University of Wisconsin – Madison; email: pfefferk@engr.wisc.edu

Abstract

The objective of this work is to evaluate the changes in microstructure and mechanical properties of S7 tool steel after surface finishing using pulsed laser micro polishing (PLμP). PLμP has been shown to effectively polish micro metallic parts, but the effects on the microstructure and resulting material properties have not been previously studied for S7 tool steel. This paper will investigate the microstructure present after PLμP and use heat transfer models to compare the observed results to the expected microstructure based on the thermal history.

Keywords: Laser polishing, microstructure, tool steel.

1. Introduction

Pulsed Laser Micro Polishing (PLμP) is a non-contact surface finishing process that uses pulses of laser irradiation to melt the surface of a metallic substrate and achieve subsequent smoothening. Previous research in PLμP has primarily focused on identifying the smoothening mechanisms at work in PLμP and working to predict and optimize the final surface roughness. These investigations have identified viscous damping of melt pool oscillations (capillary regime) and Marangoni flows caused by surface tension gradients (thermocapillary regime) as the predominant smoothening mechanisms [1]. The greatest improvements in surface finish have been achieved through the combined use of the capillary and thermocapillary polishing regimes in a multi-pass polishing scheme [2].

However, many properties of the resulting surface have yet to be thoroughly investigated including the microstructure, hardness, and residual stress state of substrate material after PLμP. These properties are expected to be directly related to the temperature distribution and cooling rate during solidification of the melt pool, which are determined by the material properties and polishing parameters. Several studies have investigated the effects of laser polishing on these properties, but work to date has focused on continuous wave laser polishing or larger melt depths (>100 μm), whereas the melt depth during PLμP is typically under 10 μm even at longer pulse durations. The large difference in melt volume is expected to greatly affect the cooling rate and therefore the final microstructure and properties.

The effect of the cooling rate on the resulting microstructure has been extremely well studied in iron-carbon systems for large scale manufacturing processes and heat treatment schedules exist for obtaining desired hardness values for a variety of steel compositions. Therefore, heat transfer models that were previously shown to accurately predict the maximum melt depth and HAZ during PLμP can also be used to predict the solidification time and resulting microstructure. Similar work has also been done in evaluating microstructure development during solid-state laser hardening [4] and in continuous wave laser polishing [5]. However, this work is typically done with much larger volumes of material than in PLμP.

Three beam diameters have been used in recent PLμP work: 30 μm, 100 μm, and 200 μm. Previous work has shown that varying the melt pool diameter may be beneficial in optimizing the final laser polished surface roughness. The current investigation will present an initial investigation into the microstructural changes occurring during PLμP under these conditions and present questions raised that will be addressed in future work.

2. Experimental Setup

2.1. Laser equipment and parameters

The experimental setup included a 1070 nm wavelength, 200 W (CW) fiber laser (SPI Lasers, Model: SP-200C-W-S6-A-B) directed into a scan head (ScanLab HurryScan 14mm) that was controlled by a ForeSight control card from LasX Industries (Fig. 1). The sample was placed on a manual z-axis stage used to account for the sample thickness and adjust the laser spot size through beam defocusing.

Three beam diameters were used: 30 μm, 100 μm, and 200 μm. The melt pool diameters measured were 15 μm, 85 μm, and 150 μm. The laser settings used for these conditions are listed in Table 1.

Table 1. Laser parameters used for three different beam diameters

Beam diameter (μm)	Pulse duration (μs)	Peak power (W)	Fluence per pulse ($*10^{-3}$ J/mm^2)
30	1.5	3.0	6.37
100	5.6	30	21.4
200	32	80	81.5

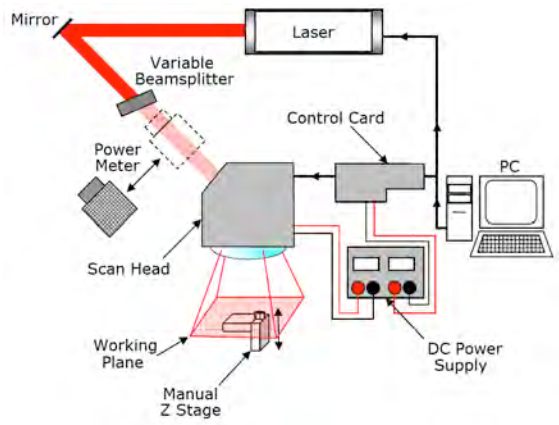

Fig. 1. Experimental setup [3].

2.2. Samples

The samples were flat ground coupons of S7 tool steel with an starting areal average roughness of S_a = 277 nm. The samples were received in a fully annealed condition. Some samples were heat treated to further harden the material.

2.3. Characterization Methods

The laser polished surfaces were examined using a white light interferometer (Zygo NewView 6300), white light focus-variation metrology system (Alicona InfiniteFocus), and scanning electron microscope (LEO 1530). The white light interferometer was used to collect accurate surface topography data and evaluate the surface roughness. The focus-variation system was used with both unpolarized and polarized light to characterize the surface appearance and also obtain surface height data. Polarized light created increased contrast in the microstructural features on the polished surface. The observed microstructural features were confirmed using the scanning electron microscope (SEM).

2.4. Thermal History Modeling

The microstructure observed after the polishing process is directly related to the thermal history of the material. Previous research has investigated and validated models that accurately predict the melt pool depth and melt pool flows using analytical and numerical multiphysics modeling (Comsol). These models have so far been used to predict the maximum melt pool depth. However, these models can be extended to obtain the entire thermal history from liquid to room temperature and predict the changes in the final microstructure. This was used to additionally explain and validate the observed final microstructure.

2.5. Hardness Testing

To evaluate the effect of laser polishing on the mechanical properties of the surface, microhardness indentation tests were performed using a nanotribometer (Anton Paar model NTR2) with normal loads of 500 mN, 750 mN, and 1 N. As a baseline, S7 tool steel samples in both the annealed and hardened condition were mechanically polished to a mirror finish (S_a < 25 nm) and tested. A hardened specimen was then laser polished with a multi-pass PLμP procedure utilizing both thermocapillary and capillary flow and the hardness was recorded.

2.6. FIB/SEM Cross-sectional Investigation

A direct investigation of the microstructure after laser polishing was conducted by using SEM with focused ion beam (FIB) capability (Zeiss Auriga) to deposit a protective carbon cap over the area of interest, then use the FIB to mill away material. The FIB milling leaves a very smooth internal wall allowing for a precisely placed cross-section view of the microstructure. An accelerating voltage of 30 keV was used with progressively smaller beam currents of 8 nA, 2 nA, 140 pA, and 80 pA to obtain a smooth wall. The wall was then imaged using secondary electron imaging.

3. Results and Discussion

3.1. Thermal History Modeling

Thermal modelling analysis of the PLμP process has already been effective at predicting the maximum melt pool depth and melt pool flows. An example temperature-time curve is shown in Fig. 2. Figure 2(a) shows that the heating and cooling follow exponential curves as expected. Also of note, the simulation was not run until complete cooling of the sample. Figure 2(b) shows the results on a logarithmic time axis, which makes the heating and cooling curves roughly linear with a constant temperature during solidification. This

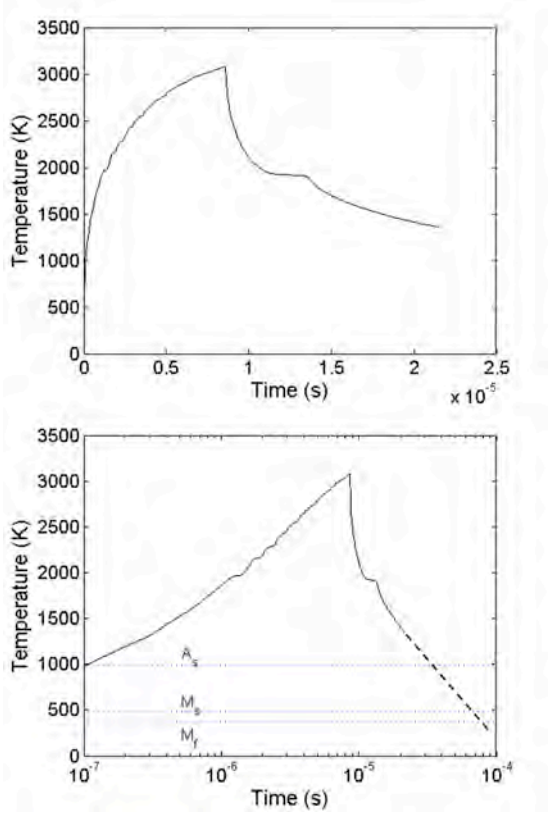

Fig. 2. Time-temperature plots of the surface of a sample experiencing heating and cooling during a single laser

log-scale plot allows a rough extrapolation of cooling to room temperature, assuming a constant exponential decay of the temperature. The plot also shows the austenizing temperature, A_s, and beginning and finishing temperatures for the martensite transformation, M_s and M_f, respectively.

This predicts that the sample will reach room temperature in approximately 100 μs after the laser pulse ends. This is significantly shorter than the time necessary to create a ferrite-cementite microstructure. This value was reached by extrapolation to save computation time and used a laser pulse duration of 10 μs, which is in the range of laser pulse durations currently used at UW-Madison.

3.2. Surface Characterization

Two methods were used to characterize the appearance of the PLμP polished surface: optical focus variation metrology and SEM. Characterization of PLμP polished surfaces using focus-variation metrology with polarized light showed that the microstructure of the resolidified surface is clearly visible after polishing in the thermocapillary regime with a large melt pool diameter of 150 μm. These features as seen in Fig. 3, included large regular circular features due to material upwelling at the edge of the melt pool (characteristic of thermocapillary flow) and smaller randomly oriented features due to the resolidified microstructure. A large beam diameter and overlap distance between laser spots was necessary for good imaging of the microstructural features with the optical system.

Higher magnification observations of the surface appearance using the SEM were done for a laser spot, line, and area using a smaller melt pool diameter of 15 μm (Fig. 4). The laser parameters used (Table 1) were chosen such that the thermocapillary flow would be minimized to reduce any surface geometry after polishing. This allowed excellent characterization of the residual surface features due to local grain structure. As in the optical surface image (Fig. 3), two types of residual surface features are clearly visible after PLμP: the edge of the melt pool and the grain structure. The grain structure of a single spot (Fig. 4a) looks very similar to that of a line of overlapped spots (Fig. 4b) and also to an area of spots (Fig. 4c).

Magnified images of a line of overlapped laser spots (Fig. 5) showed that two distinct microstructural features are present. The majority of the grain structure is characterized by grains with an approximate average diameter of 1 – 2 μm and orientation that appears random (Fig. 5b). The aspect ratio of these grains varies from roughly equiaxed to approximately 5:1. The secondary microstructural feature consists of much smaller grains, approximately 150 nm in diameter, that appear only near the edges of the solidified melt pool (Fig. 5c). Several open cracks were observed in these regions, appearing along the grain boundaries of these tiny grains. These cracks were typically under 1 μm in length.

SEM characterization further showed that larger open surface cracks, approximately 5 – 10 μm in length were observed under some processing conditions (Fig. 6). This suggests that there may be variations in the residual stress state of the resolidified or another difference in the microstructure that has not yet been identified. More analysis of the residual stress state after PLμP is necessary to explain the cause of this

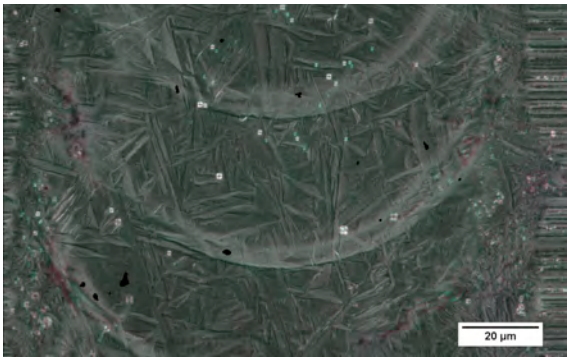

Fig. 3. Polarized light image of overlapping resolidified melt pools.

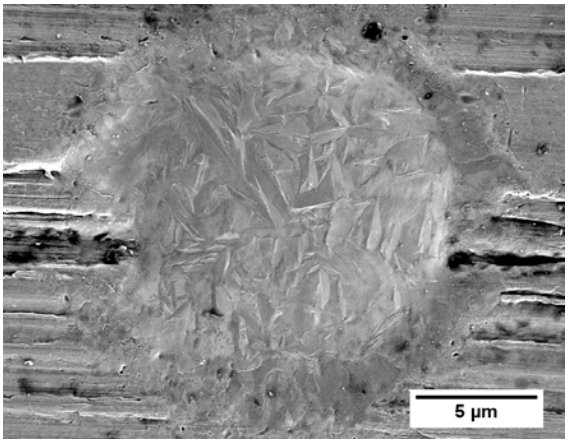

(a)

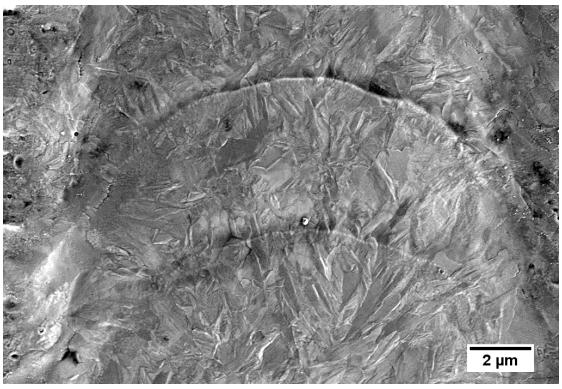

(b)

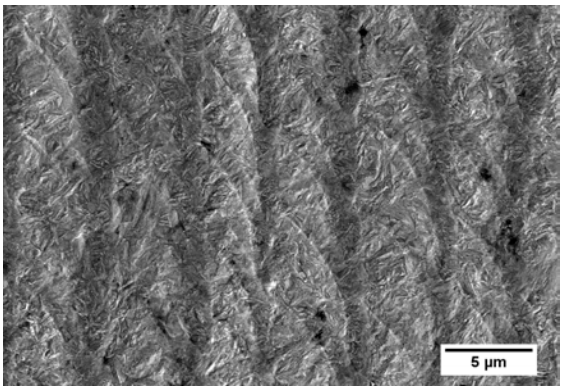

(c)

Fig. 4. SEM images of (a) individual laser spots, (b) lines of spots, and (c) areas of spots.

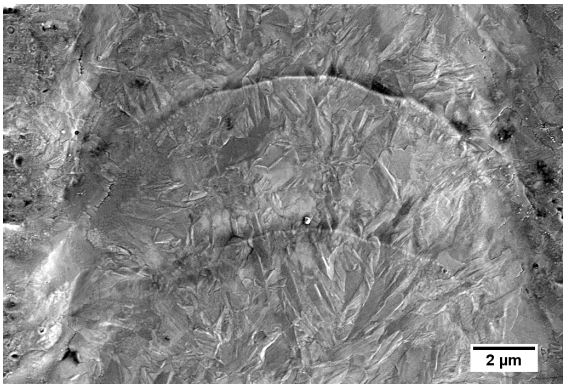

(a)

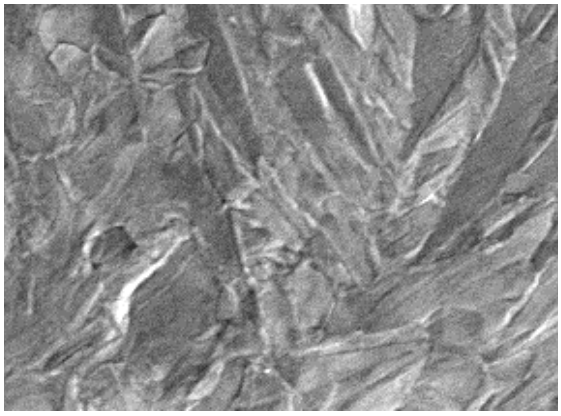

(b)

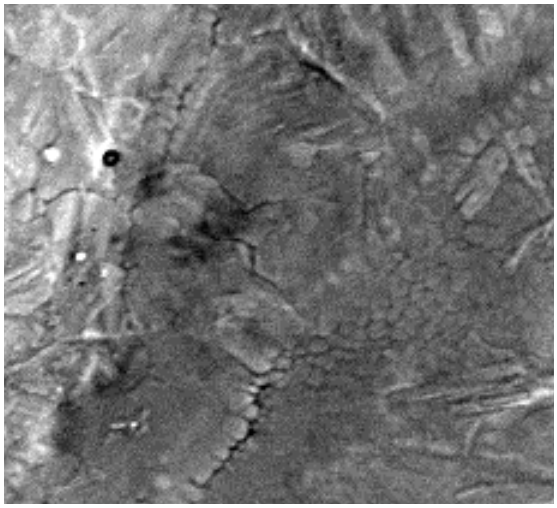

(c)

Fig. 5. Magnified SEM images of a line scan.

cracking.

3.3. FIB/SEM Characterization

In order to characterize a cross-sectional view of the microstructure resulting from PLµP, FIB/SEM characterization was done as described in the experimental methods section. The characterization was performed on a single laser spot, as shown in Fig. 7 The cross-section was made of half of a spot instead of across the entire diameter, assuming a reasonably

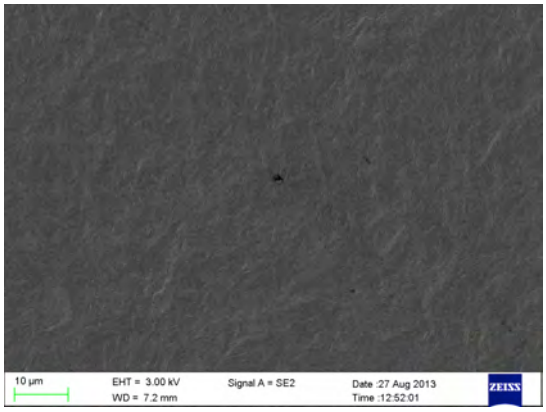

(a)

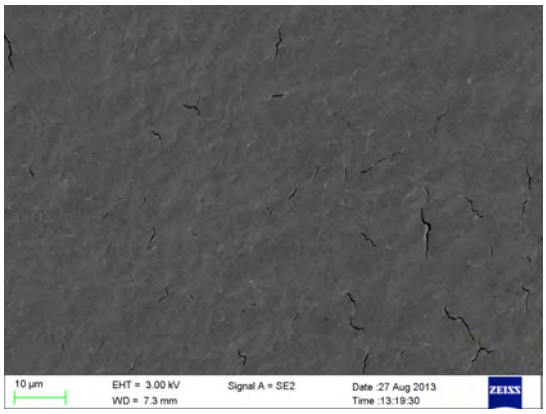

(b)

Fig. 6. SEM images of two-pass polished areas with different processing parameters on the second pass showing no cracking in (a) and significant cracking in (b).

axisymmetric structure.

A comparison of the laser melted region to the original grain structure of an as-ground region shows a distinct difference in appearance. The initial as-ground surface shows a surface layer approximately 1 µm thick of relatively small grains believed to be associated with subsurface damage caused by the grinding process (Fig. 8a). The cross-sectional view of a single laser spot shows that the laser remelted zone has a maximum depth of approximately 2 µm and has a significantly different appearance than the starting microstructure (Fig. 8b and c).

3.2. Hardness Testing

Hardness tests were performed using a spherical tip with a radius of 100 µm. The maximum force used (1N) was calculated to be 50 times higher than the load needed for plastic deformation and left an indentation of reasonable size for depth measurement using the white light interferometer with a 50x objective. Three different forces were used and the results established that the indentation area was scaling with the force as expected and the calculated hardness value did not depend significantly on the load used.

The hardness was calculated for each sample and averaged using all loading conditions (Fig 9). The samples were “S7AR” for S7 annealed round, “S7HR” for S7 hardened round, and “PLµP” for the PLµP laser

polished area. The laser polishing was done with a 3 pass approach using a 85-µm-diameter melt pool followed by a 30-µm-diameter melt pool, so the maximum melt depth was anticipated to be higher than the 2 µm depth reported for a single 30-µm-diameter melt pool. Also it is important to note that the laser polishing was done on a hardened substrate.

The scatter in the calculated hardness for samples S7AR and S7HR is small (Fig. 9): this is attributed to the ease of measuring the diameter accurately on a mechanically polished surface. The scatter for the PLµP sample was significantly larger, which is primarily attributed to the difficulty of discerning the indentation edges accurately from the surrounding surface topology. There is also an effect of the topology on the actual size of the indentation since the peak-to-valley height of the surface is on the same order as the indentation depth; the indentations varied from

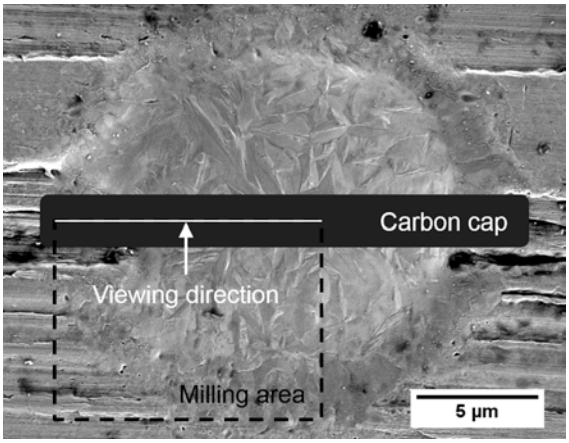

Fig. 7 Diagram of procedure used for FIB/SEM characterization of a laser spot.

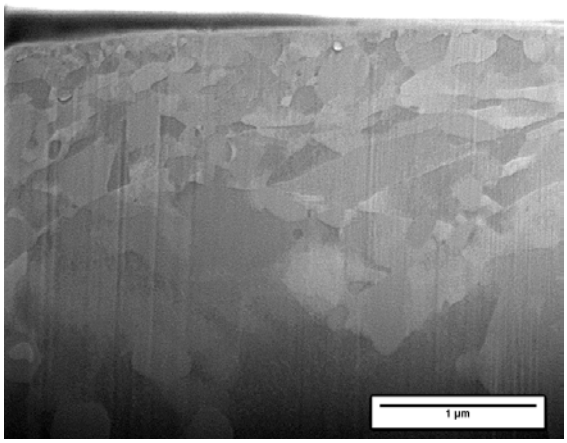

(a)

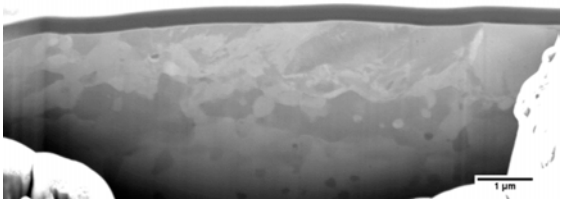

(b)

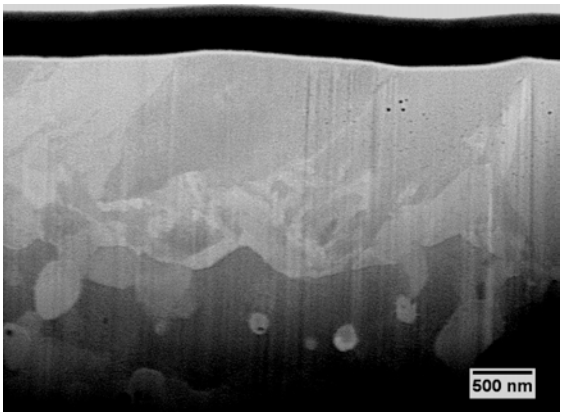

(c)

Fig. 8. SEM images of the as ground surface (a) and of a laser spot (b and c).

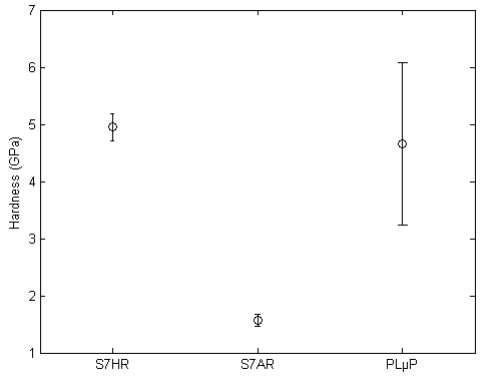

Fig. 9. Hardness values of the hardened S7, annealed S7, and laser polished (on hardened S7) surfaces.

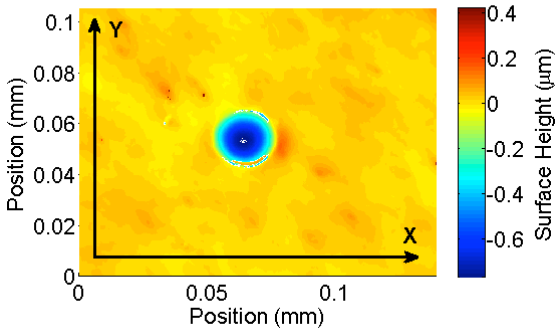

(a)

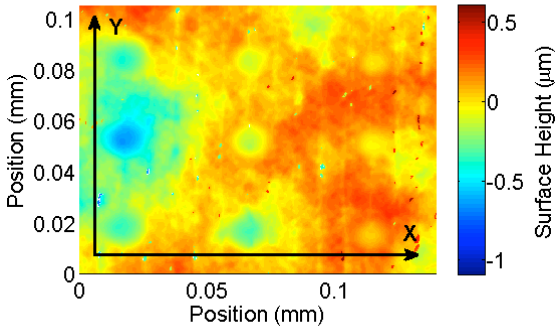

(b)

Fig. 10. White light interferometer data from an indentation in the annealed sample (a) and laser polished sample (b).

approximately 0.3 to 0.6 μm in depth depending on the load, and the surface had an average areal roughness of S_a = 72 nm and a peak to valley height of S_z = 1 μm. A comparative figure of indentations on these surfaces is given in Fig. 10.

4. Conclusions

Initial results show that it is possible to evaluate the microstructural appearance of the resolidified surface using optical and electron microscopy. In this case, the surface shows evidence of a microstructure that resembles plate martensite. This finding is supported by simulations of the laser polishing process which indicate that the cooling time is too short for diffusion-based phase transformation and should be dominated by a diffusionless martensitic transformation.

Additionally, microcracks under 1 μm in length are observed near the edges of the melt pool. High magnification SEM is needed to detect these cracks. However, it is also shown that much larger cracks, approximately 10 μm in length, can be formed under certain polishing conditions but not in others. It is inferred from this result that there may be microstructural features (*i.e.,* nanograins) that present crack initiation sites, but the final size of these cracks is dependent on the residual stress state of the material. The processing conditions are believed to play a critical role in controlling or preventing the formation of these microcracks.

Cross-sectional analysis of a single laser spot shows that the maximum melt depth is approximately 2 μm. The microstructure is characterized by a coarse structure at the surface of the melt pool (similar to the surface view) and a finer structure near the bottom of the melt pool. It is hypothesized that this indicates that nucleation of the resolidified phase began in the coolest region near the bottom of the melt pool and the solidification front progresses toward the surface. The structure quickly becomes coarser as certain grain orientations "win" over the surrounding grains.

Hardness testing of a laser polished hardened sample shows that the average hardness value is similar before and after laser polishing, although the scatter in the data from the laser polished surface is large. Also, it is not yet clear how much the indentation tests are able to separate the effect of the laser polishing from the substrate compliance.

No heat affected zone is definitively observed in the cross-sectional SEM images. It is also inconclusive whether an effect from the HAZ is apparent in the hardness tests.

Future work will be done to address the questions raised by the current work. In particular, detailed microstructural characterization and residual stress analysis will help to fully describe the resulting microstructure. Nanoindentation tests of the cross-sectional view are also being planned.

Acknowledgements

The authors would like to thank William Dinauer, Kevin Klingbeil of LasX Industries for their continued collaboration, Dr. Madhu Vadali and Chao Ma for discussions that helped further our understanding of PLμP, and Prof. Melih Eriten for the use of his nanotribometer to conduct the hardness tests.

References

[1] M. Vadali, C. Ma, N. A. Duffie, X. Li, and F. E. Pfefferkorn, "Pulsed laser micro polishing: Surface prediction model," *J. Manuf. Process.*, vol. 14, no. 3, pp. 307–315, Aug. 2012.

[2] F. E. Pfefferkorn, N. A. Duffie, X. Li, M. Vadali, and C. Ma, "Improving surface finish in pulsed laser micro polishing using thermocapillary flow," *CIRP Ann. - Manuf. Technol.*, vol. 62, no. 1, pp. 203–206, 2013.

[3] M. Vadali, C. Ma, N. A. Duffie, X. Li, and F. E. Pfefferkorn, "Effects of Laser Pulse Duration on Pulse Laser Micro Polishing," *ICOMM 2014*, 12-Mar-2012. [Online]. Available: http://digital.library.wisc.edu/1793/65473.

[4] M. F. Ashby and K. E. Easterling, "The transformation hardening of steel surfaces by laser beams—I. Hypo-eutectoid steels," *Acta Metall.*, vol. 32, no. 11, pp. 1935–1948, Nov. 1984.

[5] J. Arias, M. Cabeza, G. Castro, I. Feijoo, P. Merino, and G. Pena, "Microstructural characterization of laser surface melted AISI M2 tool steel," *J. Microsc.*, vol. 239, no. 3, pp. 184–193, 2010.